

Distribution of zeros of the S-matrix of chaotic cavities with localized losses and Coherent Perfect Absorption: non-perturbative results

Yan V. Fyodorov,¹ Suwun Suwunarat,² and Tsampikos Kottos²

¹King's College London, Department of Mathematics, London WC2R 2LS, United Kingdom

²Department of Physics, Wesleyan University, Middletown, Connecticut 06459, USA

(Dated: 03 January 2017)

We employ the Random Matrix Theory framework to calculate the density of zeroes of an M -channel scattering matrix describing a chaotic cavity with a single localized absorber embedded in it. Our approach extends beyond the weak-coupling limit of the cavity with the channels and applies for any absorption strength. Importantly it provides an insight for the optimal amount of loss needed to realize a chaotic coherent perfect absorbing (CPA) trap. Our predictions are tested against simulations for two types of traps: a complex network of resonators and quantum graphs.

PACS numbers:

One of the undisputed successes of the Random Matrix Theory (RMT) in last decades is its faithful description of scattering properties of disordered or/and chaotic cavities which have been verified by a number of experiments: distribution of conductances, delay times, resonance widths, the effects of many open channels, the consequences of preserved/violated time reversal symmetry, the presence of uniform absorption etc, see e.g. recent review articles [1–5].

Inspired by all these successes of RMT with chaotic systems, it is natural to expect that it will prove itself among essential tools for understanding of a new category of scattering problems, associated with the design of chaotic coherent perfect absorbers (CPA) [12]. CPA protocols [6, 7] have been found increasingly relevant because of our capabilities in manipulating incoming wavefront shapes in frameworks ranging from acoustics, to microwaves and optics [8–11]. They are typically weakly lossy cavities which act as perfect constructive interference traps for incident coherent radiation [6]. The potential technological applications of such CPA cavities can vary from sound protection, to microwave and antenna theory optimization and from optical switching and sensing to on-chip light modulation. Despite the broad range of technological applications the study of CPA was confined up to now to the investigation of simple (integrable) cavities. Only recently researchers started investigating the effects of complexity (chaos) in the realization of CPAs [12]. This is quite surprising since at the heart of CPA protocols are wave interference phenomena which are abundantly present in wave chaotic cavities. In fact one can further capitalize on these complex (chaotic) interferences in order to provide *universal* predictions for properties of chaotic CPA cavities.

In this paper we are utilizing the RMT toolbox in order to shed new light on the realization of chaotic CPAs with M open channels and spatially non-uniform losses. For simplicity we shall assume that the losses are described by a single point-like absorber with loss-strength γ_0 embedded inside the cavity. Specifically we provide a

detailed statistical description of the density of zeros of the scattering S -matrix which describing such chaotic CPA cavities. In particular, the number of *complex zeros* of the S -matrix that crossed the real energy axis can be interpreted as the number of “perfect absorbing states” supported by such cavities. We provide analytical expressions for the density of zeros as a function of γ_0 for a fixed M and given universality class (violated/preserved time-reversal invariance). In contrast to [12] we do not assume a weak-coupling limit, our results thus providing *non-perturbative* insights into the optimal amount of loss (perfect tuning) needed to realize a crossover of a zero from positive to negative complex energy semi-plane. Our results are tested against detailed numerical calculations using both RMT modeling and an actual wave chaotic network (quantum graphs).

Our starting point is the M -channel scattering matrix $S(E, \gamma_0)$ which connects incoming $|I\rangle$ to outgoing $|O\rangle$ wave amplitudes at a fixed real energy E via the relation $|O\rangle = S|I\rangle$, in the presence of a single localized absorber of strength γ_0 . Adjusting the approach of [13, 14] to our problem (see **Supplemental Materials**) the S -matrix can be expressed in terms of an $N \times N$ ($N \gg 1$) random Gaussian matrix H (real symmetric GOE, $\beta = 1$ or Hermitian GUE, $\beta = 2$) used to model the Hamiltonian (or, in context of classical waves, the wave operator) of an isolated chaotic cavity, and an $N \times M$ matrix W (containing the *coupling amplitudes* to M open scattering channels) satisfying, for simplicity, the relation $\sum_{l=1}^N W_{cl}^* W_{bl} = \gamma \delta_{cb}$, $\forall c, b = 1, \dots, M$ (‘equivalent channels assumption’).

The real values E for which the associated determinant $\det S(E, \gamma_0)$ vanishes define the energies of incident traveling waves for which a CPA can be realized [6]. In fact, to have CPA one has to impose a condition that the incident waveform $|I_{\text{CPA}}\rangle$ must be realized as a linear combination of channel modes with amplitudes given by the components of the eigenvector of the scattering matrix $S(E^{\text{CPA}}, \gamma_0)$ associated to a zero eigenvalue. Indeed, in this case $S(E^{\text{CPA}}, \gamma_0)|I_{\text{CPA}}\rangle = 0 = |O\rangle$ implying

there is no outgoing wave, hence CPA. The condition of zero eigenvalue in turn implies $\det S(E, \gamma_0) = 0$.

It can be shown, see **Supplemental Materials**, that in our approach the zeroes $z_n = E_n + iY_n$ of the determinant of the S -matrix are given by the N eigenvalues of the effective non-Hermitian Hamiltonian $\mathcal{H}_{eff}^{(a)}$ [12]

$$\mathcal{H}_{eff}^{(a)} = H + iWW^\dagger - i\gamma_0 |0\rangle\langle 0|. \quad (1)$$

When studying statistical properties of those zeroes, the invariance of the random matrix part H allows us to replace the matrix WW^\dagger by a diagonal one $\gamma \sum_{l=1}^M |l\rangle\langle l|$, where $|l\rangle$ is assumed to be the eigenbasis of WW^\dagger . The local point absorber is modeled by the last term in (1), with $\gamma_0 > 0$ standing for the loss- strength and the vector $|0\rangle$ (normalized as $\langle 0|0\rangle = 1$) characterizing the position of the absorber is chosen orthogonal to all channel vectors $|l\rangle$ due to physical assumption of no direct overlap between the scattering channels and the position of the absorber. For $\gamma_0 = 0$ all S -matrix zeroes are complex conjugates of the S -matrix poles (also known as 'resonances'), and because of causality they are located in the upper half complex energy plane. As, however, γ_0 increases the zeroes will be pulled down and at a certain value γ_0^{CPA} will cross the real axis. Consequently, for a given absorber strength the number of CPA states can be identified with the number of zeroes z_n 's located in the low half plane of complex energies.

In what follows we will describe the statistics of the rescaled imaginary parts of complex zeros $y_n = \beta\pi Y_n/\Delta = \pi\beta N\rho(E)Y_n$ as a function of the relative strength of the absorber $a \equiv \gamma_0/\gamma$. Here $\Delta = (\rho(E)N)^{-1}$ is the mean spacing between neighboring real eigenvalues for H close to the energy E and $\rho(E) = \frac{1}{\pi}\sqrt{1 - E^2/4}$ is the RMT density of eigenvalues.

Our main object of interest is the probability density of the *imaginary parts* for complex zeroes (whose real parts are close to the energy E) defined as $\mathcal{P}_M(y) = (N\rho(E))^{-1} \langle \sum_n \delta(y - y_n) \delta(E - E_n) \rangle_H$. Before presenting non-perturbative results valid for arbitrary coupling and absorption strength let us note that for the limit of weak coupling $\gamma, \gamma_0 \ll 1$ the limiting forms of $\mathcal{P}_M(y)$ can be found by a straightforward adaptation of Porter-Thomas first-order perturbation analysis [16, 17], see **Supplemental Materials** for a detailed exposition. This further allows to find the probability that a zero of the S -matrix crosses the real axis in the perturbative regime.

For a general coupling/absorption strengths beyond perturbation regime the density $\mathcal{P}_M(y)$ can be inferred by a judicious re-interpretation of the RMT results for *resonance* statistics obtained originally in [18], and further elaborated in [14, 19, 20]. A fully controlled *ab initio* derivation is relatively involved even for the simplest $\beta = 2$ case, and will be published elsewhere [21].

As is well-known [13, 14], as long as $N \gg M$ the main control parameters of the theory are the non-perturbative

coupling constants $1 \leq g < \infty$ and $1 \leq g_0 < \infty$ defined in terms of 'bare' values $0 \leq \gamma < \infty$ and $0 \leq \gamma_0 < \infty$ as

$$g = \left(\frac{\gamma^2 + 1}{2\pi\rho(E)\gamma} \right); \quad g_0 = \left(\frac{\gamma_0^2 + 1}{2\pi\rho(E)\gamma_0} \right) \quad (2)$$

In terms of these parameters the density of complex zeroes turns out to be given for $\beta = 2$ by

$$\mathcal{P}_M^{(\beta=2)}(y) = F_1^{(M)}(g, g_0; y) F_2^{(M)}(g, g_0; y) \quad (3)$$

where

$$F_1^{(M)}(g, g_0; y) = \frac{\theta(-y)e^{g_0y} + \theta(y)e^{-gy} \sum_{l=1}^M \frac{[(g_0+y)y]^{l-1}}{\Gamma(l)}}{(g + g_0)^M}$$

$$F_2^{(M)}(g, g_0; y) = \frac{1}{2} \int_{-1}^1 e^{-y\lambda} (g + \lambda)^M (g_0 - \lambda) d\lambda \quad (4)$$

with $\theta(x)$ being the Heaviside step function. One can easily calculate the mean imaginary part $\langle y \rangle$ for the zeros:

$$\langle y \rangle = \int_{-\infty}^{\infty} \mathcal{P}_M^{(\beta=2)}(y) y dy = \frac{\beta}{2} \left[\frac{M}{2} \ln \frac{g+1}{g-1} - \frac{1}{2} \ln \frac{g_0+1}{g_0-1} \right]. \quad (5)$$

where in the latter form the expression is also valid for $\beta = 1$ case considered later on. This formula provides a generalization of the well-known *Moldauer-Simonius* relation, see [14, 18] and refs. therein. The logarithmic divergence of $\langle y \rangle$ for $g \rightarrow 1$ or $g_0 \rightarrow 1$ reflects the characteristic power-law tails $\mathcal{P}_M^{(\beta=2)}(y) \sim y^{-2}$ in the upper/lower half plane typical for the 'perfect coupling' case.

The following remark is due here. If both parameters γ and γ_0 take values in the interval $0 \leq \gamma, \gamma_0 < 1$ the distribution (3) is asymptotically exact for all N zeroes. When $\gamma > 1$ exactly M 'broad zeroes' (i.e. located far from the real axis) separate in the upper half-plane, and following [14] we can show that their imaginary part is non-random and is given by $Y^{upper} = \gamma - \gamma^{-1} = O(1)$, see **Supplemental materials** for a derivation. The overwhelming majority of $N - M$ zeroes stay however close to the real axis at a distance of order of $1/N$ and their density is still faithfully described by the same distribution (3). The restructuring behaviour is natural to call the *zeroes self-trapping phenomenon* [12], and its analogue for the case of resonances is well-known and observed experimentally [22]. Similarly, for $\gamma_0 > 1$ a single 'broad' zero with imaginary part $Y^{lower} = -(\gamma_0 - \gamma_0^{-1})$ emerges in the lower half plane.

Use of Eq. (3) allow us to calculate the probability $\tilde{\Pi} \equiv \int_{-\infty}^0 \mathcal{P}_M(y) dy$ that, for given values of M, g and g_0 , a zero of the S -matrix crosses the real axis and hence be located in the lower half-energy plane:

$$\tilde{\Pi}^{(\beta=2)}(g, g_0) = \frac{(g+1)^{M+1} - (g-1)^{M+1}}{2(M+1)(g+g_0)^M} \quad (6)$$

From Eq. (6) we immediately infer that whenever the absorber is not '*perfectly tuned*', so that $g_0 \neq 1$, the probability $\tilde{\Pi}^{(\beta=2)}$ decays *exponentially* with the number of

open channels $M \gg 1$ – in a way similar to the perturbative regime, see **Supplemental Materials**. This is a consequence of the ‘zeroes depletion’, or ‘gap’, arising for many open scattering channels in the upper half-plane close to real axis.

A strikingly different behavior is observed in the case of “perfectly tuned” absorber $g_0 = 1$. Indeed,

$$\tilde{\Pi}^{(\beta=2)}(g, g_0 = 1) = \frac{g+1}{2(M+1)} \left[1 - \left(\frac{g-1}{g+1} \right)^{M+1} \right] \quad (7)$$

indicating that the probability to have zeroes below the real axis decays only as $1/(M+1)$, *irrespective* of the coupling strength γ of the cavity with the scattering channels. In particular, a spectral window with a large enough number of levels ($> M$) will on average contain a zero below the real axis. Hence, a single ‘perfectly tuned’ absorber dramatically increases the probability of realizing a CPA state. In fact, even in the case of slight detuning $g_0 = 1 + \frac{\delta}{M}$ (where $\delta \sim \mathcal{O}(1)$ and $M \rightarrow \infty$) we get from Eq. (7) that $\tilde{\Pi}(g, g_0) \sim \frac{g+1}{2(M+1)} e^{-\delta/(g+1)}$.

Re-interpreting the results of [19] one may also derive exact non-perturbative expressions for the distribution of zeroes for $\beta = 1$. In this case, however, the formulas are quite cumbersome, even for the simplest $M = 1$ case. In the latter case the density of zeroes in the *upper* half-plane takes the form

$$\mathcal{P}_{M=1}^{(\beta=1)}(y > 0) = \frac{1}{4\pi} \int_{-1}^1 d\lambda (1-\lambda)^2 (g+\lambda)(g_0-\lambda) e^{-2\lambda y} \mathcal{F}(\lambda) \quad (8)$$

with $\mathcal{F}(\lambda) = \int_g^\infty \frac{dp_1 e^{-yp_1}}{\sqrt{p_1^2-1}(\lambda+p_1)^2} \frac{1}{\sqrt{(p_1-g)(p_1+g_0)}} \times \int_1^g \frac{dp_2 e^{-yp_2}}{\sqrt{p_2^2-1}(\lambda+p_2)^2} \frac{(p_1-p_2)(p_1+p_2+2\lambda)^2}{\sqrt{(g-p_2)(p_2+g_0)}}$. The density of zeroes for the lower half plane $y < 0$ is obtained by replacing $y \rightarrow -y$ in the density Eq. (8) and exchanging $g \leftrightarrow g_0$ everywhere.

In the limit of a single perfect channel $g = 1$ we can further proceed and evaluate the probability $\tilde{\Pi}_1(g = 1, g_0) = 1 - \int_0^\infty \mathcal{P}(y) dy$ that for a fixed absorptive coupling value $1 \leq g_0 \leq \infty$ a given zero of the scattering matrix becomes negative. After a somewhat long calculation one arrives at the expression:

$$\tilde{\Pi}_1(g = 1, g_0) = 1 - \frac{1}{4\sqrt{2(g_0+1)}} \int_1^\infty \frac{dp}{\sqrt{(p+1)(p+g_0)}} \times \left[(g_0-1) \ln \frac{p+1}{p-1} + (4p+3g_0+1) \left(p \ln \frac{p+1}{p-1} - 2 \right) \right] \quad (9)$$

Simulations – We have tested the validity of the RMT predictions via direct diagonalization of the effective RMT Hamiltonian Eq. (1) and by an exact search of zeros of the scattering matrix describing an actual wave chaos system i.e. a complex network of one-dimensional

waveguides coupled together via splitters. The latter system has been established during the last years as a prototype model for wave chaos studies [23, 24] while its experimental realization in the microwave domain has been demonstrated by a number of groups [25–28].

The RMT model can be used to describe (in the coupled mode theory approximation [29]) a network of coupled cavities (acoustic/microwave or optical) or LC circuits which are randomly coupled with one another. The random coupling can be introduced by the randomness in the distances between the cavities (or by a random capacitive coupling in the case of LC circuits). The time-reversal invariance can be violated via magneto-optical effects in the case of electromagnetic network resonators [30] or via gyrators in the case of LC circuits [31]. The breaking of time-reversal symmetry is much more challenging in the acoustic domain but recent developments have demonstrated that it can be achieved by incorporating circulating fluid elements [32, 33].

We start with the presentation of the RMT simulations. We have considered a small window around $E \approx 0$ and we have collected at least 5000 data for statistical processing. In Figs. 1a,b,c we show the distribution of zeros $\mathcal{P}(y)$ for a GUE ($\beta = 2$) case with $M = 2$ number of channels and matrices of the size $N = 600$. The relative strength of the absorber is conveniently characterized by the ratio $a \equiv \gamma_0/\gamma$. The agreement between the numerical data and the theory is excellent when the zeroes self-trapping effect is absent (see Figs. 1a,b), for $0 < \gamma, \gamma_0 \leq 1$. For $\gamma = 2, a = 2$ Eq. (3) the predictions of RMT are still describing our data quite well on the scale of $1/N$, see Fig. 1c, in agreement with the discussion of the resonance trapping phenomenon. In the insets of Figs. 1a,b,c we summarize our results for the probability $\tilde{\Pi}^{\beta=2}(\gamma, a)$ for fixed γ -values. The numerical analysis of $\tilde{\Pi}^{\beta=1}(a)$ for the GOE case is shown in Figs. 2a,b and compared with Eqs. (S18) and (8) for weak and strong coupling respectively. Representative probability densities $\mathcal{P}(y)$ are shown in the insets of Fig. 2.

Next we proceed with the numerical analysis of zeroes for quantum graphs. The system consists of $n = 1, \dots, V$ vertices connected by B bonds. The number of bonds emanating from a vertex n is the valency v_n of the vertex and the total number of bonds can be expressed as $B = \frac{1}{2} \sum_n v_n$. The length of the bonds $l_{n,m}$ are taken from a uniform box distribution $l_{n,m} \in [l_0 - w/2, l_0 + w/2]$ where $l_0 = 1$ is its mean and $w = 1$. On each bond, the component Ψ_{nm} of the total wavefunction is a solution of the free Helmholtz equation $(i \frac{d}{dx} + A)^2 \Psi_{nm}(x) = k^2 \Psi_{nm}(x)$ where we have included a “magnetic field vector” $A = A_{nm} = -A_{mn}$ which breaks the time-reversal symmetry. At the vertices (where scattering events occur), we can introduce a δ -potential with a strength λ_n . Furthermore the wavefunction $\Psi_{n,m}$ at the vertices must be continuous and must satisfy appropriate current conservation relations. We will be assuming that losses are

concentrated in only one vertex which will have a potential strength with a negative imaginary part $-i\lambda_0''$. The system is turned to a scattering set-up once leads are attached at some of the vertices. In this case the system is described by a scattering matrix $S(k, \lambda_0'')$ where k is the wavenumber of an incident wave (for further details see [12, 23]). The zeros of the $S(k, \lambda_0'')$ matrix are then evaluated numerically.

Our numerical data for $\mathcal{P}(y)$ in two typical cases for $M = 3$ of a GUE tetrahedron graph is shown in the inset of Fig. 3a,b. The value of the scattering parameter g (associated with the real part of λ) has been extracted in two different ways from our data for graphs. The first approach invokes Eq. (5) in the absence of any loss. In this case the last term is zero and from the numerical evaluation of $\langle y \rangle$ we extract the value of g describing the coupling strength between the leads and the graph. The second approach utilizes the relation $|\langle S \rangle|^2 = \frac{g-1}{g+1}$ which by using the expression (10) from Supplemental Materials can be easily shown to be insensitive to any degree of loss incorporated in the network. Both approaches gave us the same value of $g \approx 1.65$. Then the absorption coupling g_0 (describing the loss-strength λ_0'') has been extracted using Eq. (5) – this time in the presence of absorption. In Fig. 3a we report the case with $g_0 \approx 1.07$ corresponding to (almost) perfectly tuned absorber while in Fig. 3b we report the data associated with $g_0 \approx 2.86$. From the figures it is obvious that in the former case we have a proliferation of negative zeroes as predicted by Eqs. (6,7). The effect is amplified even more in the case of chaotic graphs where the numerical data for $y < 0$ are consistently above the RMT prediction Eq. (3), see Fig. 3a. We speculate that the origin of this discrepancy is associated with the absence of a statistical gap in the resonance width distribution due to the presence of scar states, see Ref. [23, 24]. A summary of our results for $\tilde{\Pi}^{(\beta=2)}$ and various g_0 values are shown in Fig. 3c.

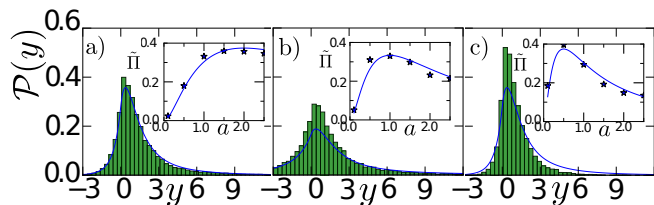


FIG. 1: (color online) Distribution of $\mathcal{P}(y)$ for a GUE RMT model with $M = 2$ and $N = 600$ (a) $\gamma = 0.5, a = 0.5$; (b) $\gamma = 1, a = 1$; and (c) $\gamma = 2, a = 2$. In all cases the solid lines are the theoretical predictions of Eq. (3). In the insets we report an overview of our results for the probability $\tilde{\Pi}(\gamma, a)$ vs. $a = \gamma_0/\gamma$. The solid lines are the theoretical predictions of Eq. (6). The symbols are the results of our simulations.

Conclusions – We have investigated the statistics of complex zeroes of a scattering matrix describing a chaotic cavity with a single point-like lossy defect. Our approach

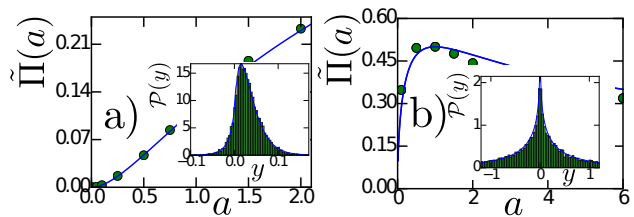


FIG. 2: (color online) Probability of negative zeroes $\tilde{\Pi}(\gamma, a)$ versus a for a GOE RMT model with (a) weak ($\gamma = 0.01, M = 4, N = 100$) and (b) strong ($\gamma = 1, g = 1, M = 1, N = 300$) coupling. The symbols represent simulations while the lines are the theoretical predictions Eqs. (22) and (9) respectively. Insets: Distribution of zeroes $\mathcal{P}(y)$ for (a) $\gamma = 0.01, a = 1$ and (b) $\gamma = 1, g = 1, a = 1$. The solid lines represent the theoretical predictions of Eqs. (18) and (8) respectively.

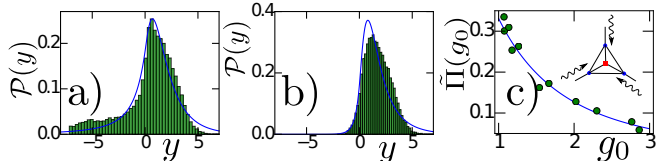


FIG. 3: (color online) Statistics of zeroes for a GUE ($A \neq 0$) tetrahedron graph (see inset in (c)) with total number of bonds $B = 6$, valency $v_n = 3$ for all vertices and $M = 3$ number of channels. The coupling strength of the graph with the lead(s) was estimated (see text) to be $g \approx 1.65$. Probability densities $\mathcal{P}(y)$ for (a) $g_0 \approx 1.076$ corresponding to (almost) perfectly tuned absorber and (b) $g_0 \approx 2.86$. The solid lines represent the theoretical predictions of Eqs. (3). (c) Probability of negative zeroes $\tilde{\Pi}(g_0)$ versus g_0 . Symbols represent the numerical data while the solid line represents Eq. (6).

assumes that the cavity is coupled with M leads and it is described by a RMT model. Using non-perturbative calculations we were able to evaluate the density of imaginary parts of S -matrix zeroes. This allowed us to calculate the probability of such a zero to move to the negative part of the complex energy plane as the loss-strength at the defect increases. We have tested our predictions both against direct numerical calculations within the RMT model and with a dynamical system described by a complex networks of coupled waveguides. Our results are "universal" and provide new insights into the problem of chaotic coherent perfect absorbers. Specifically they are directly addressing the question of the optimal amount of loss needed to realize a chaotic coherent perfect absorber. It will be interesting to extend these studies beyond universality and identify dynamical effects (like scars etc) that can further enhance the efficiency of such chaotic cavities to act as CPAs. Finally, we note that perhaps the easiest way to experimentally test our predictions for S -matrix complex zeroes is to use the correspondence elucidated in the Supplemental materials. There it is shown that in the framework of RMT such zeroes are statisti-

cally identical to zeroes of the diagonal $(M-1) \times (M-1)$ sub-block of the $M \times M$ unitary scattering matrix without absorbers. Thus we expect our results for $M=1$ should describe complex zeroes of the S_{11} element of the two-antenna device, which may be accessible by the same harmonic inversion technique used earlier in [34] for extracting resonance poles.

Acknowledgement - (Y.V.F) was supported by EPSRC grant EP/N009436/1. (S.S, & T.K) acknowledge partial support from an AFOSR MURI grant FA9550-14-1-0037 and an NSF EFMA-1641109.

-
- [1] Y.V. Fyodorov and D.V. Savin in :*The Oxford Handbook of Random Matrix Theory*, ed. G. Akemann, J. Baik and P. Di Francesco (Oxford: Oxford University Press, 2011), chapter 34, pp. 703–722 ; C.W.J Beenakker *ibid.* chapters 35& 36, pp. 723-758;
- [2] U. Kuhl, O. Legrand, and F. Mortessagne, *Fortschr. Phys.*, **61**, 414 (2013)
- [3] G. Gradoni, J.-H. Yeh, B. Xiao, T.-M. Antonsen, S.-M. Anlage, and E. Ott, *Wave Motion*, **51**, 606 (2014)
- [4] B. Dietz and A. Richter, *Chaos*, **25**, 097601 (2015)
- [5] H. Cao and J. Wiersig, *Rev. Mod. Phys.*, **87**, 61 (2015)
- [6] Y. D. Chong, L. Ge, H. Cao, A. D. Stone, *Phys. Rev. Lett.* **105**, 053901 (2010).
- [7] S. Longhi, *Physics* **3**, 61 (2010).
- [8] V. Romero-Garcia, G. Theoharis, O. Richoux, A. Merkel, V. Tournat, V. Pagneux, *Sci. Rep.* **6**, 19519 (2016).
- [9] J. Schindler, Z. Lin, J. M. Lee, H. Ramezani, F. M. Ellis, T. Kottos, *J. Phys. A: Math. and Theor.* **45**, 444029 (2012).
- [10] W. Wan, Y. Chong, L. Ge, H. Noh, A. D. Stone, H. Cao, *Science* **331**, 889 (2011).
- [11] H. Zhao, W.S. Fegadolli, J. Yu, Zh. Zhang, L. Ge, A. Scherer, and L. Feng *Phys. Rev. Lett.* **117**, 193901 (2016)
- [12] H. Li, S. Suwunnarat, R. Fleischmann, H. Schanz, T. Kottos, "Random Matrix Theory Approach to Chaotic Perfect Absorbers", accepted to *Phys. Rev. Lett.* (2016); arXiv:1701.00847.
- [13] J. J. M. Verbaarschot, H.A. Weidenmüller and M.R. Zirnbauer, *Phys. Rep.*, **129**,367 (1985)
- [14] Y. V. Fyodorov and H.-J. Sommers, *J. Math. Phys.*, **38**, 1918, (1997)
- [15] V.-V. Sokolov and V.-G. Zelevinsky, *Nucl. Phys. A*, **504**, 562(1989)
- [16] C.E. Porter and R.G. Thomas, *Phys. Rev.*, **104** 483, (1956)
- [17] Y. V. Fyodorov and D.V. Savin, *EPL*, **110**, 40006 (2015)
- [18] Y. V. Fyodorov and H.-J. Sommers, *JETP Lett.*, **63** 1026 (1996)
- [19] H.-J. Sommers, Y. V. Fyodorov, and M. Titov, *J. Phys. A: Math. Gen.*, **32**, L77 (1999)
- [20] Y. V. Fyodorov, B. A. Khoruzhenko, *Phys. Rev. Lett.*, **83**, pp. 65 (1999)
- [21] Y.V. Fyodorov and M. Poplavskiy, in progress.
- [22] E.Persson, I. Rotter, H.-J. Stöckmann, and M. Barth. Observation of Resonance Trapping in an Open microwave cavity. *Phys. Rev. Lett.* **85**, 2478 (2000)
- [23] T. Kottos and U. Smilansky, *Phys. Rev. Lett.* **85**, 968 (2000).
- [24] H. Schanz, T. Kottos, *Phys. Rev. Lett.* **90**, 234101 (2003).
- [25] M. Bialous, V. Yunko, S. Bauch, M. Lawniczak, B. Dietz, L. Sirko, *Phys. Rev. Lett.* **117**, 144101 (2016).
- [26] O. Hul, M. Lawniczak, S. Bauch, A. Sawicki, M. Kus, L. Sirko, *Phys. Rev. Lett.* **109**, 040402 (2012).
- [27] O. Hul, S. Bauch, P. Pakonski, N. Savytskyy, K. Zyczkowski, and L. Sirko, *Phys. Rev. E* **69**, 056205 (2004).
- [28] M. Allgaier, S. Gehler, S. Barkhofen, H.-J. Stöckmann, U. Kuhl, *Phys. Rev. E* **89**, 022925 (2014).
- [29] J. D. Joannopoulos, S. G. Johnson, J. N. Winn, R. D. Meade, *Photonic Crystals: Molding the Flow of Light* 2nd ed. (Princeton University Press, Princeton, NJ, 2008).
- [30] B. E. A. Saleh, M. C. Teich, *Fundamentals of Photonics*, (Wiley, New York, 1991).
- [31] JM Lee, S Factor, Z Lin, I Vitebskiy, FM Ellis, T Kottos, *Phys. Rev. Lett.* **112**, 253902 (2014).
- [32] R. Fleury, D. L. Sounas, C. F. Sieck, M. R. Haberman, A. Alú, *Science* **343**, 516 (2014).
- [33] Zh. Yang, F. Gao, X. Shi, X. Lin, Zh. Gao, Y. Chong, B. Zhang, *Phys. Rev. Lett.* **114**, 114301 (2015).
- [34] U. Kuhl, R. Höhmann, J. Main, and H.-J. Stöckmann, *Phys. Rev. Lett.* **100**, 254101 (2008)

Distribution of zeros of the S-matrix of chaotic cavities with localized losses and Coherent Perfect Absorption: non-perturbative results – SUPPLEMENTAL MATERIAL

A. S-MATRIX FORMALISM FOR SYSTEM WITH LOCAL ABSORBERS

Our goal here is to briefly describe how the presence of L localized absorbers of equal strength γ_0 (generalizations to different strength is obvious) can be taken into account in the standard RMT model of chaotic scattering introduced in [13] and described in detail in [14]. In fact, one may conveniently think of a scattering system with $M \geq 1$ open scattering channels and $L \geq 1$ local absorbers as representing jointly a system of $\mathcal{M} = M + L$ open channels, such that the corresponding $\mathcal{M} \times \mathcal{M}$ scattering matrix \mathcal{S} of the full system is unitary due to the flux conservation. From that perspective the open channels are subdivided into M *scattering* ones, described by the columns of $N \times M$ matrix W of coupling amplitudes taken, for example, as fixed orthogonal vectors satisfying $\sum_{i=1}^N \overline{W_{ci}} W_{bi} = \gamma_c \delta_{cb}$, $\forall (c, b) = 1, \dots, M$ and, similarly, L *absorptive* ones described by the columns of $N \times L$ matrix \mathcal{A} of coupling amplitudes A_{li} taken as another set of fixed orthogonal vectors satisfying $\sum_{i=1}^N A_{li} A_{mi} = \gamma_0 \delta_{lm}$, $\forall (l, m) = 1, \dots, L$. We also assume that the vector space spanned by coupling vectors A_l , $l = 1, \dots, L$ for the absorptive part is orthogonal to one spanned by vectors W_b , $b = 1, \dots, M$. In such an approach the (sub-unitary) scattering matrix $S(E, \gamma_0)$ describing the incoming/outgoing channels which were selected to support scattering is simply a $M \times M$ diagonal sub-block of the whole $\mathcal{M} \times \mathcal{M}$ scattering matrix \mathcal{S} . The matrix elements in that sub-block then have the standard form, see [13, 14]:

$$S_{ab}(E) = \delta_{ab} - 2i \sum_{ij} W_{ai}^* \left[\frac{1}{E - \mathcal{H}_{eff}} \right]_{ij} W_{jb}, \quad (10)$$

with the effective non-Hermitian Hamiltonian

$$\mathcal{H}_{eff} = H - i(\Gamma + \Gamma_A), \quad \Gamma = WW^\dagger \geq 0, \quad \Gamma_A = \mathcal{A}\mathcal{A}^\dagger \geq 0 \quad (11)$$

As is easy to check, the $M \times M$ matrix S can also be equivalently rewritten in a different form:

$$S(E) = \frac{\mathbf{1} - iK_A}{\mathbf{1} + iK_A}, \quad \text{where} \quad K_A = W^\dagger \frac{1}{E - H + i\Gamma_A} W \quad (12)$$

By using the identity $\det(1 - PQ) = \det(1 - QP)$ one can further find from (12) that

$$\det S(E) = \frac{\det(E - H + i\Gamma_A - i\Gamma)}{\det(E - H + i\Gamma_A + i\Gamma)} \quad (13)$$

The above equation makes it clear that the complex zeroes of $\det S(E)$ are eigenvalues of the non-Hermitian Hamiltonian

$$\mathcal{H}_{eff}^{(a)} = H + i(\Gamma - \Gamma_A) \quad (14)$$

Those eigenvalues are situated, as long as absorption is non-zero, i.e. $\Gamma_A \neq 0$, in both positive and negative half-planes of the complex energy. When studying their distribution in the complex plane one can safely assume the matrices Γ and Γ_A to be diagonal, due to statistical rotational invariance of the Hamiltonian matrix H . Choosing $L = 1$, so that the matrix \mathcal{A} is rank-one, and denoting the eigenvector corresponding to its only non-vanishing eigenvalue as $|0\rangle$ for convenience we arrive at (1).

B. PERTURBATIVE TREATMENT IN THE WEAK-COUPLING REGIME

When both $\gamma, \gamma_0 \ll 1$ the anti-Hermitian part in Eq. (1) can be treated as a perturbation of the Hermitian part H . In this regime one expects the zeroes to be located in the vicinity of the real axis in such a way that their 'height' in the complex plane satisfy $Y_n \ll \Delta$. First order perturbation theory results in replacing $E_n \rightarrow z_n = E_n + iY_n$ with

$$Y_n = \langle n | WW^\dagger | n \rangle - \gamma_0 |\langle n | 0 \rangle|^2 = \gamma \sum_{l=1}^M |\langle n | l \rangle|^2 - \gamma_0 |\langle n | 0 \rangle|^2 \quad (15)$$

where $\{|n\rangle\}$ are the eigenvectors of H . In the following we assume that E_n is close to $E = 0$, so that the appropriately rescaled variables are $y_n = \beta N Y_n$. The probability density $\mathcal{P}_M(y) = \langle \delta(y - y_n) \rangle_H$ in this case can be further evaluated by using the fact that the projections $\langle n | l \rangle = u_l + i(\beta - 1)v_l$ of the eigenvectors of H in any arbitrary basis, for large $N \gg 1$, can be effectively replaced with a set of independent, identically distributed mean-zero Gaussian-distributed variables u_l, v_l with variance $1/\beta N$. This implies, in particular, $\langle |\langle n | l \rangle|^2 \rangle_H = 1/N$ for both $\beta = 1$ and $\beta = 2$ and all $l = 0, \dots, M$. In this way one arrives to the mean value of the rescaled imaginary part of zeroes:

$$\langle y \rangle_H = \frac{\beta}{2} [2\gamma M - 2\gamma_0] \quad (16)$$

Remembering that in the perturbative regime when $\gamma, \gamma_0 \ll 1$ we have $g = \frac{1}{2}(\gamma + \gamma^{-1}) \approx (2\gamma)^{-1}$ we see that (16) matches exactly the large- g asymptotics of the Moldauer-Simonius relation (5).

Further Fourier-transforming the δ -function one can easily perform the averaging over eigenvector components and find the distribution of the rescaled imaginary parts as

$$\mathcal{P}_M^{(\beta)}(y) = \int_{-\infty}^{\infty} \frac{dk}{2\pi} \frac{e^{iky}}{(1 + 2ik\gamma)^{\beta M/2} (1 - 2ik\gamma_0)^{\beta/2}}, \quad (17)$$

which by further manipulations can be represented in a manifestly real form:

$$\mathcal{P}_M^{(\beta)}(y) = C_M^{(\beta)} \frac{e^{-\frac{y}{2\gamma}}}{2\gamma} \int_{-\frac{y}{2\gamma_0}}^{\infty} dt \left(at + \frac{y}{2\gamma} \right)^{\beta \frac{M}{2} - 1} \frac{e^{-(a+1)t}}{t^{1-\beta/2}} \theta(t) \quad (18)$$

where $C_M^{(\beta)} = \frac{1}{\Gamma(\beta/2)\Gamma(\beta M/2)}$ and $\theta(t)$ is the Heaviside step function. Eq. (18) is a generalization of the Porter-Thomas distribution for M open channels, and is reduced to it in the limit $a \rightarrow 0$ [16].

At this point it is worth briefly discussing how the exact non-perturbative distribution (8) takes the form (18) in the weak coupling limit $g \gg 1, g_0 \gg 1$. In such a limit one can see that the main contribution in (8) comes from the domain $p_1 \gg 1$ whereas $p_2 \sim \lambda \sim 1$. In such a limit the integrals drastically simplify and one arrives at the following expression:

$$\mathcal{P}_{M=1}^{(\beta=1)}(y > 0) = \frac{\sqrt{g_1 g_0}}{2\pi} \Phi(y) \int_g^{\infty} \frac{e^{-yp_1} dp_1}{\sqrt{(p_1 - g)(p_1 + g_0)}} \quad (19)$$

where

$$\Phi(y) = \frac{1}{2} \int_1^{\infty} \frac{e^{-yp_2} dp_2}{\sqrt{p_2^2 - 1}} \int_{-1}^1 \frac{(1 - \lambda^2) e^{-2\lambda y} d\lambda}{(\lambda + p_2)^2} \quad (20)$$

$$= K_0(y) \left(\cosh(2y) - \frac{\sinh(2y)}{2y} \right) + K_1(y) \sinh(2y)$$

where the last integral was evaluated in [17]. The above manipulations did not assume anything about the value of y . However, the typical values of the variable y in the perturbative regime are small: $y \sim \gamma \ll 1$, implying $\Phi(y \ll 1) \approx 1$. The remaining integral over p_1 is by a straightforward change of variables reduced to form featuring in (18) with $M = 1$, $\beta = 1$, $g = (2\gamma)^{-1}$ and assuming $y > 0$, thus confirming the expected correspondence.

Equation (18) allow us to evaluate the probability $\tilde{\Pi}_M(a) \equiv \int_{-\infty}^0 \mathcal{P}(y) dy$ that, for given a and M , a zero of the S -matrix crosses the real axis. For $\beta = 2$ one finds

$$\tilde{\Pi}_M^{(\beta=2)}(a) = \left(\frac{a}{1+a} \right)^M \quad (21)$$

while for $\beta = 1$ we have:

$$\tilde{\Pi}_M^{(\beta=1)}(a) = 1 - 2\Gamma\left(\frac{M+1}{2}\right) C_M^{(\beta=1)} \int_0^{\arctan \frac{1}{\sqrt{a}}} (\cos \theta)^{M-1} d\theta. \quad (22)$$

which in the small a -limit becomes:

$$\tilde{\Pi}_M^{(\beta=1)}(a) = K_M a^{M/2} + \dots, \quad K_M = \frac{\Gamma\left(\frac{M+1}{2}\right)}{\Gamma(1/2)\Gamma\left(1 + \frac{M}{2}\right)}. \quad (23)$$

Equation (23) is relevant for CPA protocols, which usually are concerned with situations where the absorber is weak enough to absorb by itself the incident waves.

Next let us consider a spectral strip in the complex plane (say around $E = 0$) parallel to the imaginary axis, with a width W so that it contains on average $L = W/\Delta$ complex zeroes. Furthermore let us denote with L_a the number of those zeroes which are below the real axis. These are the number of "perfect absorbing" states for a given set of parameters. Its mean then is given by $\langle L_a \rangle = L \tilde{\Pi}_M^{(\beta)}(a)$, while L_a itself has the binomial distribution:

$$\mathcal{P}^{(\beta)}(L_a) = \binom{L}{L_a} \left(\tilde{\Pi}_M^{(\beta)}(a) \right)^{L_a} \left(1 - \tilde{\Pi}_M^{(\beta)}(a) \right)^{L-L_a} \quad (24)$$

Specifically for $\beta = 1$, we can calculate the probability to have zero "perfect absorbers" in the $a \ll 1$ limit. Using Eqs. (23,24), we find

$$\mathcal{P}^{(\beta=1)}(L_a = 0) \approx \left(1 - K_M a^{M/2} \right)^L \approx e^{-K_M L a^{M/2}} \quad (25)$$

which allow us to identify the scaling of the minimal $a = \gamma_0/\gamma$ associated with at least one CPA state. Specifically by setting $L \sim N$ and requesting that $\mathcal{P}(L_a = 0) = O(1)$ we get that $a_{\min} \sim N^{-2/M}$. The large value of a_{\min} for $M \gg 1$ is a direct consequence of the fact that, in this limit, the density of zeroes for $\gamma_0 = 0$ is strongly depleted. Hence one needs larger values of γ_0 in order to drive such zeroes through the real axis.

C: 'ZEROES TRAPPING' PHENOMENON: CALCULATIONS FOR $M = 1$.

Let us give a derivation of the imaginary parts of 'broad' zeroes Y^{upper} and Y^{lower} for the simplest non-trivial case $M = 1$. To this end, consider the quantity $\sum_{n=1}^N Y_n$ where summation goes over *all* N complex zeroes of the effective Hamiltonian $\mathcal{H}_{eff}^{(a)}$. In the case of $M = 1$ such quantity must satisfy the sum rule: $\sum_{n=1}^N Y_n = \text{Im Tr} \mathcal{H}_{eff}^{(a)} = \gamma - \gamma_0$. On the other hand, the right hand side of the sum rule must remain unaffected after an ensemble average. Therefore we have

$$\gamma - \gamma_0 = \sum_{n=1}^N \langle Y_n \rangle = N \int_{-2}^2 \langle Y_n \rangle \rho(E) dE = \Phi(\gamma) - \Phi(\gamma_0), \quad (26)$$

where $\langle \dots \rangle$ indicates an ensemble average, $\rho(E) = \frac{1}{\pi} \sqrt{1 - E^2/4}$ is the density of states and $\Phi(\gamma) = \frac{1}{2} [\gamma + \gamma^{-1} - |\gamma - \gamma^{-1}|]$. In order to perform the integration in Eq. (26) we expressed $\langle Y \rangle$ in terms of its rescaled variable $\langle y \rangle$ which in the case of 'narrow' (i.e. with the typical imaginary part of order of $1/N$) zeroes has been evaluated in Eq. (5). The last step for the evaluation of the integral is to substitute from Eqs. (2) the energy-dependent functions g, g_0 appearing in Eq. (5).

We find that as long as both $\gamma, \gamma_0 < 1$, the right hand side of Eq. (26) is $\gamma - \gamma_0$ i.e. equal to the left hand

side. On the other hand, if either (or both) $\gamma, \gamma_0 > 1$ the result of the integration (right hand side of Eq. (26)) is different from one predicted by the exact sum rule (left hand side of Eq. (26)) by an amount $Y^{upper} = \gamma - \gamma^{-1}$ or $Y^{lower} = -(\gamma_0 - \gamma_0^{-1})$, respectively. This "deficit" is exactly due to the fact that we did not consider in the integration the contribution of 'broad zeroes' which are not captured by the distribution $\mathcal{P}_2^{(\beta=2)}(y)$ and thus by Eq. (5).